ingegneria sismica
International Journal of Earthquake Engineering
Anno XLIII - Num. 2 - 2026

Study on Intellectual Tiredness Harm Identification and Early Alarm in the Automobile and Steel Structure Industries That Includes Time Feature Analysis

Qiuyan Li[1,*], *Qingyun Ge*[2], *Caimei Li*[3] *and Fulian Yang*[4]

[1] Hunan Communications Polytechnic, Changsha, 410132, Hunan, China
[2] West Anhui University, Lu'an, 237012, Anhui, China
[3] Gates Winhere Automobile Water Pump Products (Yantai) Co., Ltd., 712000, Shandong, China
[4] West Anhui University, Lu'an, 237012, Anhui, China

SUMMARY: *In the identification of fatigue damage for critical load-bearing parts of automobiles and welded connection points in steel structures under random cyclic loads, a time lag exists. To address this, this paper proposes an intelligent industrial fatigue damage identification and early warning method that incorporates time-series feature analysis.First, a multi-source fatigue time-series dataset covering both automotive and steel structure scenarios is established. Information such as strain, vibration, acoustic emission, and load is uniformly converted into sliding-window samples and categorized into four damage stages according to the fatigue evolution process.Next, a joint model is developed, combining multi-scale time-series encoding, domain-consistent constraints, a damage identification head, and one risk regression head, for realizing the coordinate optimization of discrete stage recognition and continuous risk output. Based on this foundation, a smoothed early warning index and a continuous trigger mechanism are brought in, in order to change the model's output result into a stable early warning signal which is suitable for being directly used in online monitoring. Experimental outcome indicate that the put forward method attains recognition accuracy of 97.8% and 96.9% in automobile and steel structure situation, one by one, with Macro-F1 scores of 0.972 and 0.964. It maintains good robustness under conditions of noise and missing channels, with an average early warning lead time of 14.1%.Case studies further demonstrate that the proposed method can detect the temporal precursors of microcracks from their initiation to the stable propagation stage at an early stage, showing significant potential for real-time deployment in industrial monitoring workflows.*

KEYWORDS: *fatigue damage detection; temporal feature analysis; automotive components; steel structures; intelligent early warning*

1 Introduction

For automobile chassis connecting pieces, wheel end load bearing parts and steel structure welding seams, they are under the combined action of random loads, impact loads and environment interferences in a long time. The tiredness harm normally grows step by step via stress gathering, tiny crack starting, steady spreading, and key break-down. The real difficult problem in industry places not in verifying the generation of cracks after the event happens, but

*lqy884420@163.com
https://doi.org/10.65102/is2026749
Published: 30 April, 2026

in whether enough stable precursor information can be got out from continuous time-series responses before damage turns obvious. For car parts, the detection that is late brings about the decrease of rigidity, the growth of noise, and the cutting down of safety margins; As for steel structure works, when welding toe cracks and abnormal strain heat points are not handled in time, they therefore often accumulate together to bring about a drop of joint load bearing ability and unplanned stop of production. To establish a unified frame for fatigue damage recognition and early warning aiming at these two kinds of objects, it has obvious engineering value.

In the domains of fatigue monitoring and structural health monitoring, data-driven methods have developed from the early classification relying on single statistical features to deep feature modeling that can hold long time series, multi-sensor data and complex working situations. Correlative literature reviews show that the merits of deep learning within structural health monitoring mainly reside in its capability to automatically depict high-dimensional sensor data, carry out nonlinear recognition for complicated damage modes, and hold the possibility for online renewals; however, its working effect still mostly relies on data quality, the reliability of labels, and the adaptability of different scenes [1, 2]. This indicates that for effectively putting intelligent monitoring means into fatigue situations in the automobile and steel structure industries, relying only on static identification models which are trained under single-object, single-condition situations is far from enough.

In the automotive sector, research focus has gradually shifted from traditional post-life assessment to damage state tracking and prediction during operation. Wen et al. [3] combined digital twins with power density theory for fatigue life prediction of front axle housings in off-road vehicles; Venturini et al. [4] established a digital twin framework for automotive steel wheels to enable failure identification under accelerated fatigue testing; Heindel et al. [5] utilized a virtual sensing approach for fleet monitoring to achieve dynamic condition identification and fatigue monitoring; further work has shown that the scattering transform can reduce the computational burden of online fleet-level fatigue damage monitoring at a limited cost [6]. Such research has propelled automotive fatigue monitoring from offline test analysis toward in-service sensing; however, since the modeling objects often target individual components or single load spectra, significant obstacles remain when transferring these models to other steel load-bearing structures.

In the domain of steel constructions, the combination of digital twins, multi-source sensing, and data-pushed identification is also getting faster. The authors Jiang et al. [7] put forward a digital twin-based framework for predicting fatigue life of steel bridges, and Nhamage et al. [8] Scholars have utilized digital twin technology to carry out the description work on the fatigue condition of railway steel bridges. With regard to the welding-made parts, Li et al. [9] utilized deep learning to cluster acoustic emission (AE) data, enabling on-site crack assessment of bridge welded joints; Ma et al. [10] further combined deep learning with AE monitoring for weld damage monitoring; and Zhu et al. [11] proposed a machine learning-based fatigue life prediction scheme for E36 steel welded joints. Meanwhile, Yang et al. [12] and Sadeghian et al. [13] demonstrated the application potential of deep learning models in damage identification for steel load-bearing members from the perspectives of complex strain fields and the time-series response of steel beams, respectively. On the whole, the domain of steel constructions has built up a firm base on the technology of sensing; however, the models are generally constructed around individual structural objects, which causes that they are hard to be directly applied to industrial fatigue situations-such as those in the automobile field-that are similar but not completely isomorphic.

Along with the fatigue data-guided research going deep into more fine-grained object layers, public and special use datasets have already started to come forth. Chen et al. [14] released a deep learning dataset for predicting the fatigue life of metals under multi-axial loading; Deng

et al. [15] constructed a dataset on the fatigue performance of welded joints; and Hamada et al. [16] systematically summarized the main modeling approaches for machine learning in fatigue life prediction. These works have solved the problem of "many methods yet dispersed data" in fatigue study and hence show that intelligent fatigue analysis is moving from single case research to a stage that gives the same weight to data arrangement, task definition and model verification. However, most current data collections concentrate on life reverting or single-object material property forecasting, and support for continuous time-series damage recognition and on-line early alerting still is not enough. Especially, the aspect which lacks is a unified sample arrangement method which connects automotive parts and steel structure parts.

With regard to the modeling of time sequences, studies on automobile and steel parts have already started to probe into the combining of convolutional networks, recurrent networks and Transformer networks. Zhang et al. [17] proposed a multi-axis fatigue life analysis method for automotive components combining LSTM and CNN, demonstrating that deep time-series features can improve fatigue modeling performance under complex loading conditions.In the field of structural damage detection, Lin et al. [18] achieved cross-domain structural damage detection through deep transfer learning; Wang and Xia [19] further utilized reweighted adversarial domain adaptation to enhance target domain recognition performance; Giglioni et al. [20] and Lu et al. [21] demonstrated the value of domain adaptation for cross-structural generalization in bridge monitoring scenarios.Meanwhile, Lei et al. [22] introduced modal sensitivity into physics-guided deep learning, improving recognition stability under unseen damage modes. As for steel welded structures, the research made by Schubnell et al. [23] A study of transfer learning by s and has proven that pathways for transferable usable knowledge can be found between similar welding feature spaces. With respect to the description of signals in the periods of microcrack and crack expansion, Shi [24] and other researchers and the research group of Liu [25] have respectively proved that, the combination of acoustic emission and machine learning can effectively reflect the changes which belong to different stages in the fatigue damage of steel.

Although the studies which have been mentioned above have laid an important foundation for this present paper, four key gaps still exist. First, the automotive parts and steel structure components are usually established models separately, hence the absence of a united fatigue time-sequence arrangement method for both these situations therefore makes models hard to share the capability of describing early damage patterns. Second, the current research puts more stress on the classification of final state or the estimation of life, but it still has insufficiency in continuous risk output and stable trigger mechanisms for online early warning, and particularly lacks the design of early warning indices which can be directly integrated into industrial monitoring work flows. Third, although many methods make use of time-series models, they still regard multi-sensor information as simple connected inputs, and thus cannot adequately construct the model for the fusion of local pulses, phase transitions and cross-scale evolution. Fourth, sensor noise, missing channels, and sample distribution shifts-these are problems that often appear when cross-scene deployment is carried out-greatly damage the stability of models, which are challenges that cannot be avoided in industrial environments.

According to the above discussion, the core problem this paper discusses can be concluded like this: In the fatigue working situations of the automobile and steel structure industries, how can a united recognition framework be built which deals with long-term tendency analysis, cross-situation feature matching, and the stability of online early warning? This framework must let the model not only accurately judge the present damage phase but also provide engineering-related early warning information before key damage takes place. For solving this problem, the present paper carries out the following works. First, as for automotive parts and steel structure welded parts, a united multi-source fatigue time sequence sample arrangement

method is built to realize alignment and label mapping of strain, vibration and acoustic emission information on the same time scale. Second, hence we put forward a fatigue damage identification and early warning model which integrates multi-scale time coding, domain-consistent restriction terms and a risk regression header, thus enabling representation study to at the same time support both state identification and early warning output. In the end, by means of dual-scenario comparison experiments, module ablative research, and individual case analyses, we have verified the comprehensive effect of the method we put forward on three aspects, which are identification accuracy, cross-scenario transfer capability, and early warning advance time.

2 Methods

2.1 Dual-scenario Data Acquisition and Sample Construction

This present article hereby constructs an integrated investigation model which serves for two representative kinds of industrial fatigue research objects. One kind includes steel load-bearing parts in automobile application situations, containing the front subframe connection region, wheel-end force positions, and welding transition regions. The other kind includes welding stress nodes in steel structure situations, like welding H-beam connecting parts, stiffened connecting regions, and local hot-point zones. Although these two kinds of objects have differences in service environments, structural scales and load forms, they have common characteristics in the process of fatigue evolution, for example, the increase of strain fluctuations, partial stiffness decrease, the enhancement of acoustic emission activity, and the continuous growth of crack-related parameters. Hence, this research does not process the two kinds of objects separately, but on the contrary first arranges them consistently on the data collection stage, and then builds directly alignable time-series windows on the sample level.

In the automobile working condition, a hydraulic follow-up tiredness experiment platform is utilized to carry out loading, wherein the load is constituted by a combination of a random road frequency spectrum and a local reinforcing block frequency spectrum. This method does the simulation for the cyclic loading situations of a vehicle which is under complex working conditions. In the steel structure situation, a servo loading system is used for carrying out alternating constant-amplitude and variable-amplitude cycles, therefore the key point is placed on the damage accumulation stages which are near weld toes and within stiffened connection regions. Both two kinds of situations use four kinds of channels: strain, vibration, acoustic emission, and load reference. The strain channels are employed by people to describe partial stress variations; the vibration paths show entire dynamic responses and rigidity changes; the acoustic emission passageways confirm the activity degree after microcrack starts; and the load reference channels make external excitation and structural responses to be aligned together. In order to guarantee that following analyses will not get influence from differences of collecting devices, the original data has the processing of abnormal value elimination, baseline offset adjustment, band-pass filtration, time aligning, and uniform sampling again before it enters the stage of model construction.

In the stage that data are collected, this research uses a method of sliding window with fixed length to cut the continuous signal into units of analysis that are at the window level. Each individual window contains 8 synchronous signal channels and 1,024 data dots, possessing a 50% overlapping rate and a unified sampling frequency of 2 kHz. This method is established upon two points of thinking: firstly, the window length must be enough to hold local influences, short-time undulations, and groups of local affairs; Second, keeping a certain overlapping between window pieces can decrease the discontinuousness of information which exists at the

boundaries of phases. After sliding window segmentation has been finished, every window keeps information about its connected sample, experiment situation, loading step, and location on the life axis, therefore to help later independent sample sorting, step recognition, and early warning statistical calculation. For the purpose of not depending only on one alone measurement to divide fatigue stages, this thesis builds a comprehensive damage index which acts as a window-level monitoring standard, what can be seen in Equation (1).

$$d_i = \omega_1 \bar{a}_i + \omega_2 \left(1 - \bar{k}_i\right) + \omega_3 \bar{e}_i, \quad \omega_1 + \omega_2 + \omega_3 = 1 \tag{1}$$

where,d_i is the comprehensive damage index for the th window i, $\bar{a}_i$ is the normalized crack characteristic, $\bar{k}_i$ is the normalized stiffness retention rate, $\bar{e}_i$ is the normalized acoustic emission activity, and ω_1, ω_2, ω_3 represent the weights of the three types of information. The sample stages are classified into four categories: d_i<0.20 is classified as the intact stage, 0.20≤d_i<0.40 is classified as the microcrack initiation stage, 0.40≤d_i<0.70 is classified as the stable propagation stage, and d_i ≥0.70 is classified as the critical damage stage.This classification is not based directly on single-window instantaneous values; instead, a 5-window majority-voting smoothing is first performed on the specimen's time axis, followed by the identification of stage boundaries based on continuous segments, to reduce label contamination caused by boundary window jitter. The specimen, channel configuration, and window sample sizes for the two scenarios are shown in Table 1.

Table 1: Constitution and Categorization of Dual-Scenario Weariness Time-Ordered Data Collections

Scenario	Critical Object	Sample Size	Monitoring Channels	Unified Sampling Frequency	Payload Block/ Working Segment	Sliding Window Sample Size	Training/ Validation/ Testing
Automotive	Front subframe connection area, wheel load-bearing parts	38	8	2 kHz	456	92,160	23 / 7 / 8 samples
Steel Structure	Welded H-beam joints, stiffening connection areas	26	8	2 kHz	288	57,600	16 / 5 / 5 samples

In Table 1, the working conditions of automotive and steel structure have differences in the quantity of test pieces, load blocks and sliding window samples; however, these two types all have identical sampling frequency, channel bandwidth and window length, hence they provide a unified foundation for modeling. With regard to the organization of specimen-level data, the present study uses strict independent division, in order to prevent that different time parts of the same specimen enter the training set and the testing set at the same time. In the automotive situation, our work obtained a total of 38 samples, 456 loading blocks, and 92,160 effective windows; In the working condition of steel structure, we have obtained altogether 26 test samples, 288 loading blocks, and 57600 effective observation windows. The training set, validation set and test set were split by 6:2:2 proportion on the specimens. For the purpose of illustrating the unified organization of samples in the two scenarios, you can look at Figure 1.

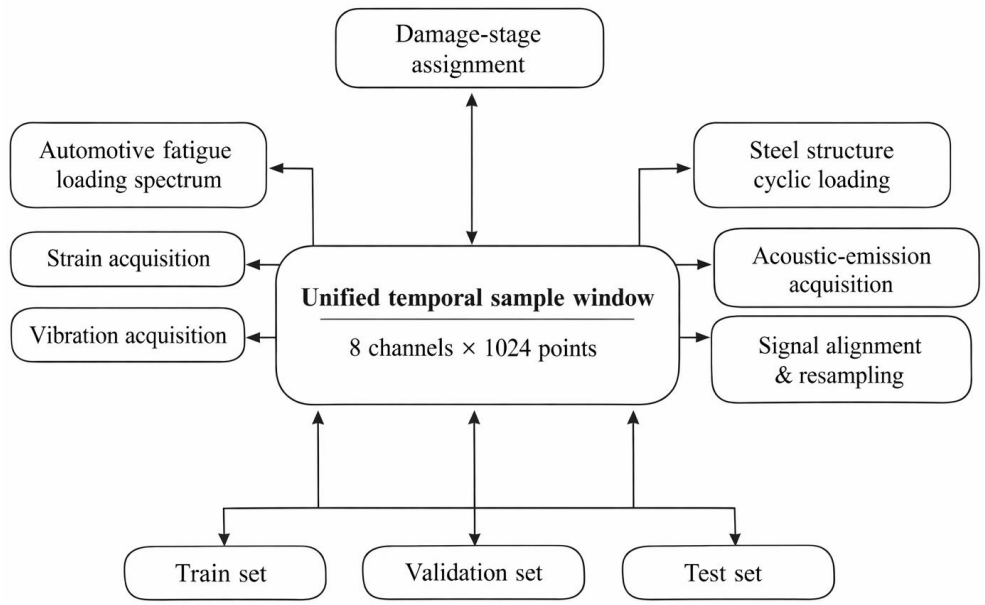

Figure 1: Data Organization and Sample Construction Mechanism for Dual Scenarios.

In Figure 1, the automotive and steel structure samples were not split into two separate workflows during the preprocessing stage but instead shared the same "acquisition-alignment-window-label mapping" path, laying the foundation for subsequent cross-scenario recognition and unified early warning.

2.2 Temporal-feature fusion and fatigue-state identification strategy

After the unified sample construction work is finished, this method puts emphasis on two key problems: first, how to at the same time extract information concerning local anomalies, phase transitions, and cumulative degradation from continuous response signals; second, how to carry out the guarantee of comparability between automobile parts and steel structure connection nodes under the same recognition frame.

Features inside the window main reflect the instant condition inside a certain analysis unit. On the domain of time, root mean square (RMS), mean drift, peak factor, kurtosis, and amplitude from cycle to cycle are extracted for the characterization of load disturbances, local impacts, and the degree of response discretization; In the frequency domain, we extract main frequency shift, inter-band energy ratio, high-frequency energy percentage and spectral center to recognize modal response changes which are caused by stiffness decrease and local crack expansion; The event-domain characteristics are obtained from the sound emission channel and contain event number, accumulated energy, mean event gap, and high-energy event ratio, which are utilized to catch the raised event activity after microcrack begins. After we in parallel extract these three kinds of features, the information about stress, dynamics and crack activity can at the single-window scale be retained at the same time.

Features that lie inside one single window only are still not enough, because the core key of fatigue damage does not only lie in "whether there exists an abnormal situation at a certain time point", but also lies in "whether the abnormal situation continues, accumulates, and develops from one stage to another stage". According to this thinking, this paper further builds the evolution characteristics between windows. In concrete terms, the change speed, local motion average value, local discrete degree, and single-direction increase duration are computed among neighboring windows and local window sequences. The changing rate can find fast growths inside short time periods; the moving average method has the function of

suppressing occasional peak values; the difference of local variation can separate stable increasing from sharp changes; and the persistence of monotonic growth thus determines whether one feature is continuously moving in the direction of damage. In the automobile work situations, the change of road frequency spectrums and impact modules frequently bring about instantaneous peak values; In the scenarios of steel structures, cracks that have just entered the propagation phase more commonly manifest themselves as slow and continuous increases. The evolutionary features between the windows are specifically made for separating these two types of phenomena.

Given the objective differences between objects in the two scenarios in terms of geometric scale, connection types, and external loads, this paper does not feed all extracted features directly into the classifier but first performs a cross-scenario consistency screening. The screening criteria include three aspects: first, whether the same feature exhibits a consistent damage direction in both automotive and steel structure scenarios-that is, whether its direction of change remains stable as damage progresses; second, whether the feature maintains low variability across repeated specimens;third, whether it exhibits separability across the four stages. After screening, 26 core features were ultimately retained for the classifier, including 11 time-domain features, 9 frequency-domain features, and 6 event-domain features. The purpose of this step is not to reduce the dimensionality per se, but to eliminate features that are only incidentally effective in a specific scenario and difficult to reuse across objects.

In terms of the classifier architecture, this paper divides the method into four functional layers.

(1) Feature normalization and intra-group fusion layer, used to compress features of different dimensions to a unified scale and to perform intra-group aggregation of time-domain, frequency-domain, and event-domain information;

(2) Stage Classification Layer: This layer provides window-level classification into four states: intact, initiation, propagation, and critical;

(3) Risk Ranking Layer: This layer determines the relative risk positions of windows along the same test specimen's lifespan axis;

(4) The scenario correction layer, which mitigates discrepancies between the vehicle and the steel structure caused by differences in load magnitude, structural scale, and sensor amplitude.

Here, "scenario correction" does not involve redefining the classification rules for the two object types, but rather suppressing the interference of source differences on stage identification while maintaining consistent stage boundaries.

The promotion of this distinguishing method is mainly manifested in two aspects. Firstly, this method does not any longer take fatigue identification as a separated classification of a static window, but instead it processes local features and continuous change inside the identical classification framework, hence it achieves earlier distinguishing between real degradation and accidental abnormal situations. Second, the method brings in cross-scenario consistency filtration before features go into the classifier, hence ensuring that the final classification standards depend as much as possible on measurement indicators which are "valid in both scenarios" rather than on response modes particular to a single object kind. In order to explain the corresponding relation between time feature analysis and tired condition identification, therefore please look at Figure 2.

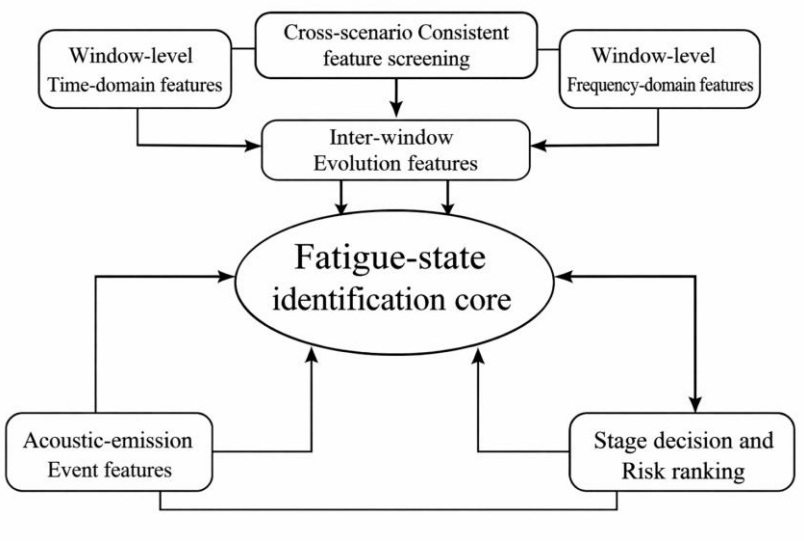

Figure 2: Mechanism of Temporal Feature Analysis and Fatigue State Recognition.

In Figure 2, intra-window features answer the question "What information does the current window contain?", inter-window evolution features answer "Is this information changing continuously?", and cross-scenario consistency features answer "Which information is suitable for adoption by both scenarios." On this basis, stage classification and risk ranking are no longer two isolated outputs but jointly serve subsequent stable early warning.

2.3 Early-warning rule and experimental protocol

After we have finished the work of window-level identification, this paper further carries out the transformation of the identification results into actionable early-warning signals. The core point here rests in whether the early warning has enough stability and whether it can give a reaction as early as it is possible and hence will not enlarge incorrect alarms. For this purpose, this paper has built a smoothed early-warning index which is based on the comprehensive damage index, which is shown in Equation (2).

$$E_t = \lambda d_t + (1-\lambda)\frac{1}{w}\sum_{j=t-w+1}^{t} d_j \tag{2}$$

where E_t is the smoothed early-warning value for the th window t, d_t is the composite damage index for the corresponding window, w is the smoothing window length, and λ is the current window weight. In practice, the system does not directly issue an alarm for a single high-value window; instead, it requires that E_t exceed the scenario threshold for three consecutive windows before determining a stable early warning. This design is primarily intended to suppress two common sources of false triggers in these scenarios: short-term impact peaks in automotive scenarios and localized sensor fluctuations in steel structure scenarios. Thresholds are set using a validation set calibration strategy, with a warning threshold of 0.58 for automotive scenarios and 0.55 for steel structure scenarios.

To verify whether this early warning rule is truly suitable for engineering applications, the experimental protocol focuses on four aspects: identification accuracy, early warning capability, robustness, and deployment efficiency. The identification section primarily addresses whether the four-stage window can be reliably distinguished, so three metrics-Accuracy, Macro-F1, and AUROC-are used; the early warning section primarily addresses whether the system can issue

alarms as early and as reliably as possible, so the average early warning lead time, average number of cycles until critical damage, and false alarm rate are used.Here, the average early warning lead time is defined as the proportion of remaining lifetime between the first stable alarm point and the critical damage point; the average early warning lead cycle count is calculated directly as the difference in cycles between the alarm point and the critical point. Combining these two metrics simultaneously reflects both "whether a lead time exists" and "whether the lead time is of engineering significance."

A total of five methods were included in this comparison: Random Forest, 1D-CNN, LSTM, CNN-LSTM, and Time-Series Transformer.Among these, Random Forest represents a traditional discriminative approach based on manually engineered features; 1D-CNN and LSTM represent typical approaches for local pattern extraction and time-series dependency modeling, respectively; CNN-LSTM is used to examine the effects of combining local features with time-series structures; and Transformer is used to compare modeling capabilities for long-range dependencies and multi-feature interactions. All methods employ the same input window, the same specimen segmentation, and the same maximum number of training iterations to prevent comparison biases caused by differences in data specifications. In the methods presented in this paper, the training phase uses uniform feature inputs and uniform stage label definitions; parameters are not designed specifically for any single scenario.

For the further evaluation of the method's adaptive ability under on-site conditions, the present paper carries out two kinds of expanding verification experiments. The first kind category include of noise perturbation experiment tests, which is that simulate recognition retention ability capabilities under the conditions of transmission signal being contaminated contamination, structural vibration interference, and environmental noise getting increased increased environmental noise through by progressively decreasing reducing the signal-to-noise ratio. The second classification includes absent channel experiments, which assess the influence of partial data missing upon recognition outcomes through randomly covering some channels. Besides, this article at the same time records the quantity of parameters and single-window inference time delay, to judge whether the model can satisfy the demands of online updating. If a method obtains good performance in main outcomes but has obvious instability on noise, absent channels or inference efficiency, its application in industry is still not enough. Hence, these verification experiments are not supplementary but make up components of the same importance as the core identification outcomes. The organizational connections inside the experimental plan must strictly correspond to the figure marks in the main body of the text. For illustrating the relationships between experimental arrangement, comparison methods, and assessment interfaces, please look at Figure 3.

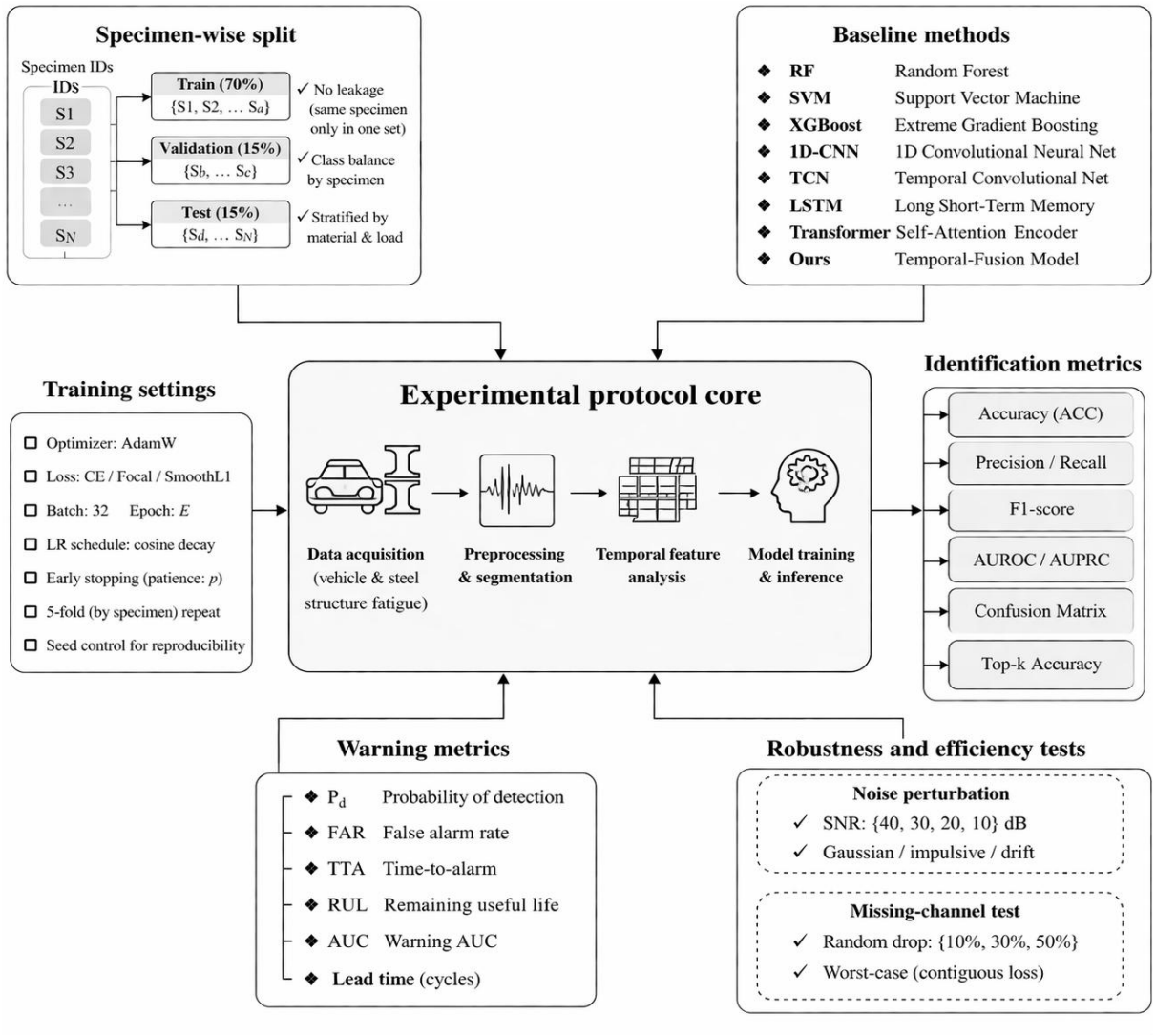

Figure 3: Experimental Protocol, Comparison Strategy, and Evaluation Mechanism.

Figure 3 illustrates the connections between sample-level segmentation, baseline method groups, training metrics, recognition metrics, and early warning metrics.

3 Results and Discussion

3.1 Overall Identification Performance and Cross-Scenario Generalization

After completing unified training and validation, this section first addresses two questions: how effective is the proposed method in the dual scenarios of automotive and steel structures, and does the shared temporal representation truly improve cross-scenario generalization? A comparison of the main results of different methods on the dual-scenario fatigue damage identification task is shown in Table 2.

Table 2: Comparison of core outcomes for various approaches on the two-scenario tired harm recognition work

Method	Automotive Accuracy / %	Automotive Macro-F1	Automotive AUROC	Steel Structure Accuracy / %	Steel Structure Macro-F1	Steel Structure AUROC
RF	89.4	0.881	0.934	86.7	0.852	0.918
1D-CNN	93.1	0.921	0.961	91.5	0.904	0.949
LSTM	93.8	0.928	0.966	92.1	0.911	0.953
CNN-LSTM	95.6	0.947	0.978	94.4	0.936	0.969
Time-Series Transformer	96.4	0.956	0.983	95.1	0.944	0.975
Proposed Method	97.8	0.972	0.991	96.9	0.964	0.986

Table 2 shows that our method achieves the best results in both scenarios. In the automotive scenario, Accuracy, Macro-F1, and AUROC reached 97.8%, 0.972, and 0.991, respectively; in the steel structure scenario, they reached 96.9%, 0.964, and 0.986, respectively.Compared to the state-of-the-art baseline, the Time-Series Transformer, the automotive scenario saw a 1.4 percentage point increase in Accuracy, a 0.016 increase in Macro-F1, and a 0.008 increase in AUROC; the steel structure scenario saw a 1.8 percentage point increase in Accuracy, a 0.020 increase in Macro-F1, and a 0.011 increase in AUROC.These results indicate that the combination of multi-scale temporal fusion and domain-consistent constraints simultaneously improves both class discrimination and cross-scenario stability. The precision-recall curves and normalized confusion matrices are shown in Figure 4.

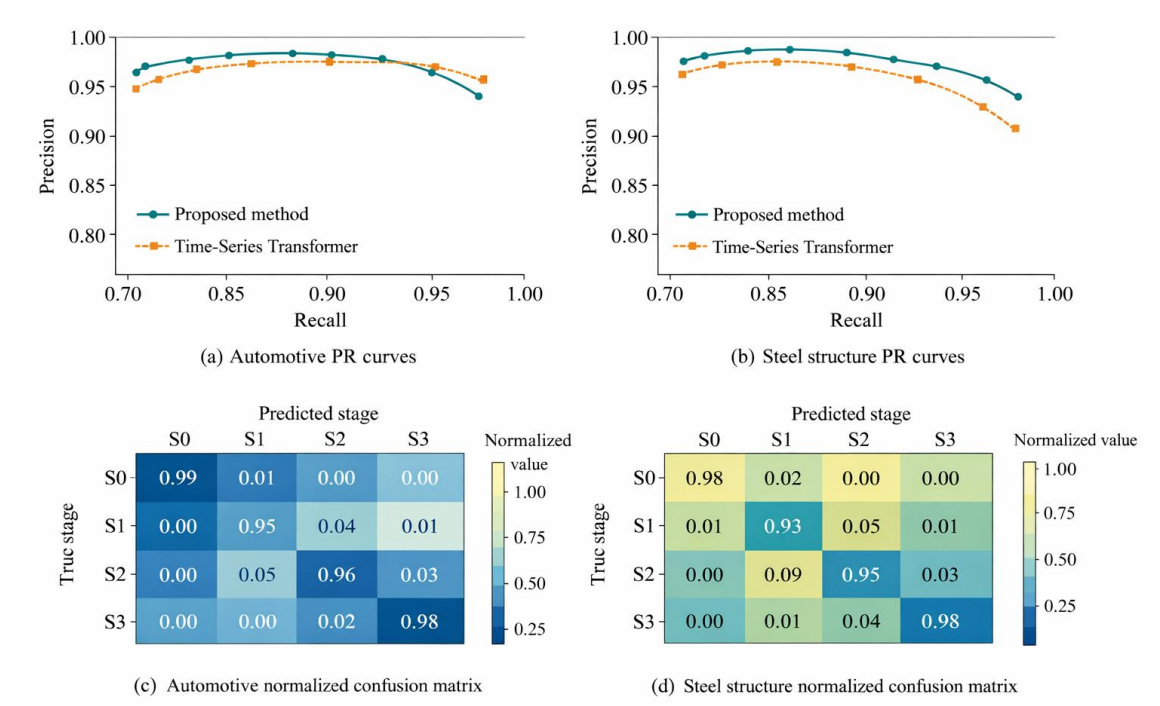

Figure 4: Main precision-recall curves and normalized confusion matrices for the dual scenarios.

In Figure 4(a), when Recall is fixed as 0.90, the precision value of our method in the automobile use scenario is still 0.955, while the corresponding value of the Time-Series Transformer is 0.888; In Figure 4(b), the corresponding Precision numerical values for the steel structure scene are 0.939 and 0.861, respectively. This result shows that the model holds a low false positive rate when it reduces false negatives to the smallest degree. This characteristic is especially of high value for fatigue warning tasks, because on-site use situations give priority to stable judgments when recall conditions are at high level.

The error distribution is further demonstrated by confusion matrices, which is displayed in Figure 4(c) and 4(d). Under the situation of automobile domain, the diagonal elements corresponding to four kinds of states S0, S1, S2, S3 are respectively 0.989, 0.948, 0.955, 0.979; and regarding the working condition of steel structure, these values are 0.982, 0.931, 0.947, and 0.975, separately. The mistakes are mainly gathered among neighbor steps, for example, S1 and S2. For instance, on the automotive working situation, the ratios of S1 that wrong classified into S0 and S2 are 0.028 and 0.020, each separately, hence in the steel structure situation, the corresponding ratios are 0.034 and 0.029. By comparison, wrong classifications across different stages between S0 and S3 are nearly zero, hence this shows the model holds a stable hold on the dividing lines between the complete and key stages; the real difficult part is still the boundary window in which microcrack starting changes to stable spread. The capability of shared representation is further been shown in Figure 5.

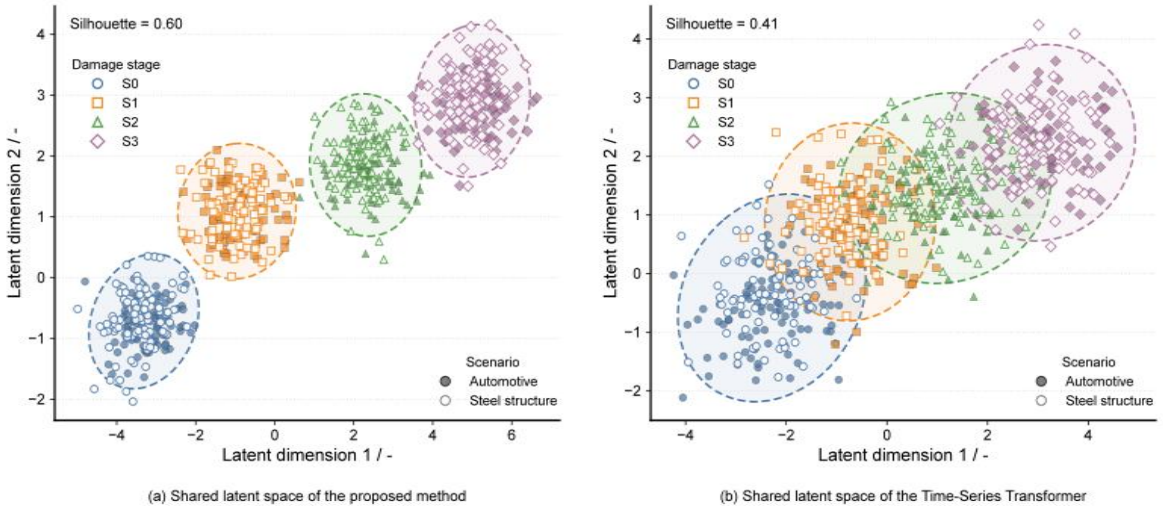

Figure 5: Damage stage separation in the shared temporal representation space.

In Figure 5, samples from different scenarios but at the same damage stage show significant overlap within the same cluster, while clear separation is maintained between different stages.Measured by the contour coefficient, the representation space of our method scores 0.60, while the Transformer baseline scores 0.41. This phenomenon indicates that the domain-consistency constraint does not weaken stage discriminability; rather, it makes the latent space less dominated by scene origin and more organized by damage evolution stages. For subsequent cross-object reuse, this means the model does not need to relearn all low-level temporal patterns for every new structure.Furthermore, in Figure 5(a), S0 and S3 are located at opposite ends of the embedding space, while S1 and S2 are sequentially distributed in the intermediate transition zone; the four types of samples form a relatively stable hierarchical arrangement along the damage evolution direction. Within the same stage, although the vehicle and steel structure samples use different labels, they are intermixed within their respective cluster ellipses, indicating that scene differences do not dominate the final representation.In contrast, in Figure

5(b), there is more pronounced boundary diffusion between S1 and S2, as well as between S2 and S3 in the Transformer model, with particularly extensive overlap in the intermediate stages. This is consistent with the phenomenon of misclassification clusters in adjacent stages observed in Figure 4.In other words, the advantages of our method lie not only in more compact clusters but also in more stable stage intervals and more thorough cross-scene mixing, making it easier for early damage windows to maintain distinguishability in the shared space.

3.2 Ablation, Robustness, and Efficiency Analysis

After confirming the overall performance, this section further examines whether the internal improvements to the model are truly effective and addresses whether the model can remain stable under conditions of noise, missing channels, and online deployment. The module ablation and efficiency results are shown in Table 3.

Table 3: Key module ablation, cross-scenario transfer, and real-time efficiency results

Method	Automotive Accuracy/%	Automotive Macro-F1	Automotive AUROC	Steel Structure Accuracy/%	Steel Structure Macro-F1	Steel Structure AUROC
RF	89.4	0.881	0.934	86.7	0.852	0.918
1D-CNN	93.1	0.921	0.961	91.5	0.904	0.949
LSTM	93.8	0.928	0.966	92.1	0.911	0.953
CNN-LSTM	95.6	0.947	0.978	94.4	0.936	0.969
Time-Series Transformer	96.4	0.956	0.983	95.1	0.944	0.975
Proposed Method	97.8	0.972	0.991	96.9	0.964	0.986

In Table 3, the full model achieves the best performance across all three core metrics: Overall Macro-F1, Cross-domain F1, and Mean warning lead ratio. After removing the multi-scale temporal branch, the Overall Macro-F1 drops from 0.968 to 0.942, a decrease of 0.026, indicating that local impulse features and medium-to-long-term decay trends indeed need to be modeled simultaneously.After removing the cross-domain consistency loss, Cross-domain F1 drops from 0.943 to 0.901, a decrease of 0.042-the most significant reduction among all modules-indicating that the cross-scenario representation sharing capability primarily stems from this constraint.After removing the monotonicity constraint, the Mean Warning Lead Ratio decreased from 14.1% to 8.7%; after removing the warning fusion head, it further decreased to 6.1%. This indicates that the latter two improvements primarily affect the lead time and stable triggering of warnings, rather than merely influencing static classification results. The robustness results are consistent with the ablation trends, as shown in Figure 6.

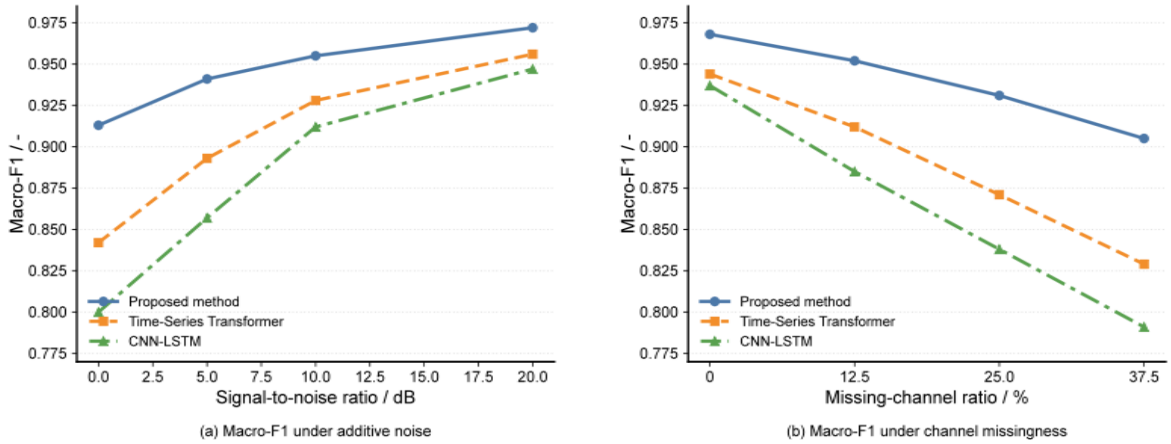

Figure 6: Robustness curves under noise perturbations and missing channel conditions.

In Figure 6(a), as SNR decreases from 20 dB to 0 dB, the Macro-F1 of our method drops from 0.972 to 0.913, a decrease of 0.059; the Time-Series Transformer drops from 0.956 to 0.841, a decrease of 0.115;and the CNN-LSTM drops from 0.947 to 0.799, a decrease of 0.148. In Figure 6(b), when the proportion of missing channels increases to 37.5%, our method still maintains a Macro-F1 of 0.905, while the Time-Series Transformer and CNN-LSTM drop to 0.829 and 0.791, respectively.These results demonstrate that the model exhibits higher robustness against noise contamination and local sensor failures. This is attributed to the multiscale branches, which preserve the temporal structure of the remaining channels when some channels degrade, while the domain-consistency constraint reduces over-reliance on the statistical distribution of a single scene.

In terms of deployment cost, the full model has 4.32 million parameters, with an average inference latency of 18.6 ms per window-an increase of only 1.4 ms compared to the non-multiscale version-yet it yields a 0.026 improvement in Overall Macro-F1 and a 3.9 percentage point increase in early warning rate.With the current settings of a 1,024-point window, 2 kHz sampling rate, and 50% overlap, the system refresh cycle is 0.256 s. The inference overhead is significantly lower than the online update cycle, meeting real-time monitoring requirements. In other words, the additional complexity of our method is manageable and primarily yields two harder-to-achieve capabilities: cross-scenario recognition and stable early warning.

Therefore, the conclusions drawn from the results in this section are clear: multi-scale temporal fusion is responsible for enhancing representational completeness, domain-consistent terms are responsible for improving cross-scenario generalization, and monotonicity constraints and the early warning fusion head are responsible for transforming recognition results into earlier and more stable alarm signals.

3.3 Case Study, Error Sources, and Deployment Implications

After validating the overall metrics and module functions, this section turns to specific case studies to examine how early warning signals are formed, where errors primarily originate, and why the model holds value for industrial deployment. The early warning process for a typical automotive test case is shown in Figure 7.

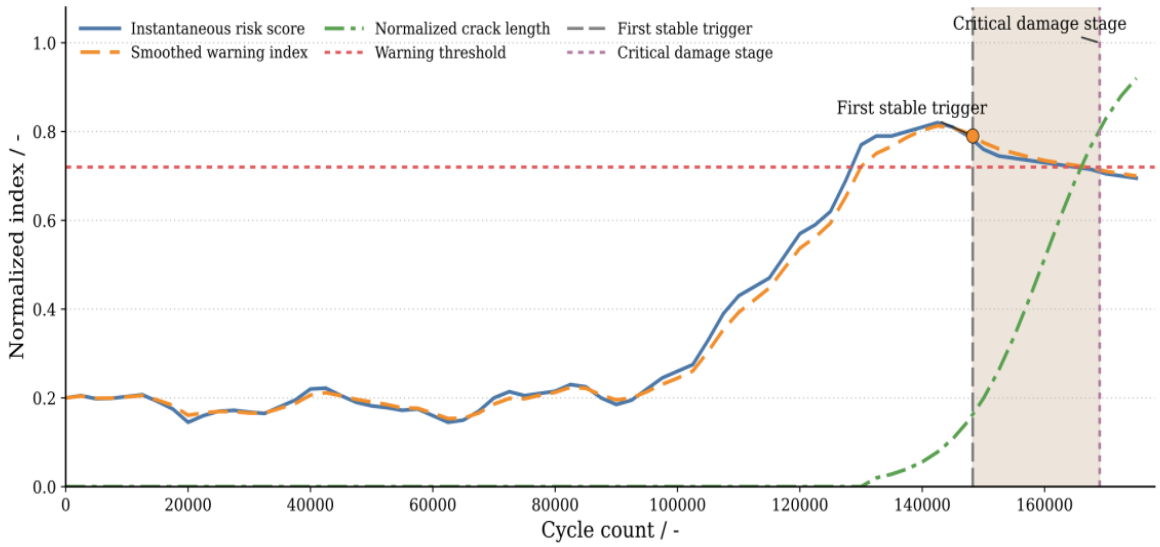

Figure 7: Evolution of warning scores and threshold triggering for a typical automotive test case.

One key character of automobile situations is the stable property of early warning starting, which just like what is displayed in Figure 7. In Figure 7, the instant risk value starts to increase stably near 1.40×10^5 cycles, although it still has many partial peak points; the smoothed early warning index has obvious convergence toward this tendency, and it first passes the threshold in a stable manner at 1.4825×10^5 cycles. The corresponding critical harm point appears at 1.6900×10^5 cycles, a difference of 2.075×10^4 cycles, it corresponds to a percentage of residual life of 12.3%. This shows that the monotonicity restriction and the smoothing start mechanism effectively reduce the disturbance of high-frequency undulations to the alarm logic, hence making the early warning signal more closely match the real degeneration inflection point instead of being pushed by separate impulse signals. The steel structure situation demonstrates the corresponding relation between continuous risk and physical harm, which is shown in Figure 8.

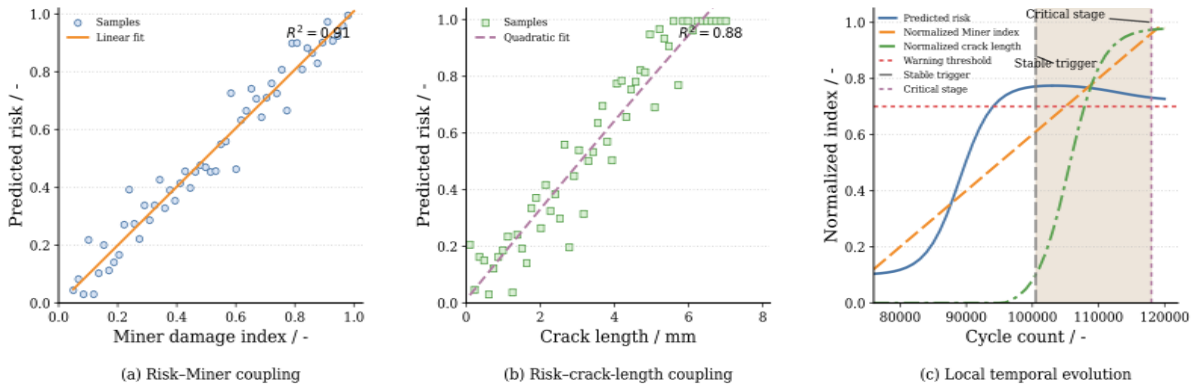

Figure 8: Coupling relationship between predicted risk, Miner damage index, and crack length in a typical steel structure specimen.

In Figure 8(a), the determination coefficient for the fitting between forecast risk and the Miner damage index is 0.91; In Figure 8(b), the coefficient of determination that is for the fitting between the predicted risk and the crack length is 0.89. Two kinds of results all show that the

risk output does not simply copy the phase classification labels, but on the contrary provides a continuous quantitative response for the damage accumulation process. Figure 8(c) is further showed by us that, in one common steel structure test sample, the first stable early warning happened at 1.005×10^5 cycles, and the critical damage point lies at 1.190×10^5 cycles; this warning has been issued when there are still 1.85×10^4 cycles left ahead, which corresponds to 15.5 percent of the total remaining life. When we compare with the automobile situation, this sample shows a higher rate of early warning. This, therefore, is because the Miner exponent and crack length display a more continuous, monotonic rise in the latter periods, hence making it easier to establish a stable mapping that belongs to the risk head.

The origins of error can also be gotten explained through the combination of Figure 4 and Figures 7–8. In Figure 4, the great part of wrong classifications are gathered in the stage which is next to S1 and S2, hence this shows that the model's most sensitive area lies in the initiation-to-propagation transition zone. Through combining Figure 7 together with Figure 8, we can discover that this phase commonly displays itself as a rise of the acoustic emission event rate, strengthened local strain drift, and gradual growth of crack length; however, the time point of changes in these three kinds of signals is not completely synchronous, thus it brings about short-term labeling unstability between the adjacent windows. In the automobile work situations, mistakes happen more often close to the temporary changes which are brought by impact loads, therefore, in the steel structure work situations, mistakes are more usual during the time when cracks have just come into stable extension but their geometry sizes have not yet got fast growth. Because of this above reason, the processed early warning index is hence more suitable than the immediate risk score to act as the final alarm trigger.

From the angle of deployment arrangement, Figures 7 and 8 are not only presenting single separated cases but explain how the method which this paper talks about can be combined into the work flows of industry monitoring. First, continuous risk outputs can directly be connected with existing threshold logic, maintenance sorting, and work order starting systems, hence reducing policy changes that are caused by transformation between discrete classifications. Second, the common expression on two situations lowers the dependence on big-scale marked data when new things are brought in, hence building a basic base for transfer ability between car parts and iron structure parts. At last, the 18.6 ms single-window time delay in Table 3, together with the surplus service lead time that surpasses 10% displayed in Figures 7–8, therefore together prove that this method satisfies the deployment standards of being "calculationally doable, can realize early detection, and gives stable warnings."

4 Conclusion

Based on the fatigue monitoring requirements for automotive steel load-bearing components and steel structure welded joints, this paper establishes a unified dual-scenario temporal recognition and early warning framework, and completes systematic validation from sample organization and feature selection to risk warning.The results show that the proposed method achieves Accuracy of 97.8% and 96.9%, Macro-F1 of 0.972 and 0.964, and AUROC of 0.991 and 0.986 in the automotive and steel structure scenarios, respectively, with overall recognition performance superior to that of all comparison methods.

(1) This present paper has established a unified method for organizing temporal samples, which at the same time covers objects of automotive and steel structure kinds. It maps strain, vibration, acoustic emission, and load reference signals onto a unified window dimension, and thus uses a comprehensive damage index to define four-stage labels, therefore it gives a unified data foundation for cross-scenario fatigue identification.

(2) The method which we put forward obtained a cross-domain F1 score of 0.943 in tasks

across different scenarios, with an average time that early warning leads of 14.1%. What we speak specifically is that the early warning lead time values for common automotive test samples and common steel structure test samples are 12.3% and 15.5%, one and the other. it has the inference delay of a single window that is 18.6 ms. This has proven that this method not only raises the accuracy of stage recognition but also has very strong online early warning ability and the feasibility of being deployed.

(3) The present research mainly puts emphasis on steel load-bearing components and has not yet included extra situations like aluminum alloys and composite materials; hence the future work needs to further enlarge the kinds of objects, and bring in adaptive threshold renewing and on-spot increment learning mechanisms to promote transfer stability in long-term working situations.

About the Author

Li Qiuyan in 1981 was given birth in Shangqiu, Henan, China. She obtained her master's degree through the completion of studies at Central South University. At current stage, she holds the post of Director of the Teaching and Research Group for the Automobile Making and Examination Technology Specialized Field inside the Automobile Engineering College, Hunan Communication Polytechnic College. Her main study direction lies in mechanical design and manufacturing.

Ge Qingyun take birth in Linyi, Shandong, China, in the year 1979. She has gotten a master's diploma from the Chang'an University which is in China. She at the present time holds a work position at the School of Architecture and Civil Engineering, West Anhui University. Her main direction of research lies in the intelligent construction of algorithms and steel-concrete combined structures.

Li Caimei was born in Linyi, Shandong, China, in 1975. She earned a bachelor's degree from Yantai University in China. She currently works at Gates Winhere Automobile Water Pump Products (Yantai) Co., Ltd. Her primary research focus is structural design.

Yang Fulian was born in Shangqiu, Henan, China, in 1979. She earned a master's degree from Henan Polytechnic University in China. She is currently working at the School of Architecture and Civil Engineering, West Anhui University. Her primary research focus is engineering mechanics.

References

[1] Jia, J., & Li, Y. (2023). Deep learning for structural health monitoring: Data, algorithms, applications, challenges, and trends. Sensors, 23(21), 8824.

[2] Cha, Y. J., Ali, R., Lewis, J., et al. (2024). Deep learning-based structural health monitoring. Automation in Construction, 161, 105328.

[3] Wen, C.-K., Liu, Z.-Y., Wu, G.-W., et al. (2023). Digital twin-driven fatigue life prediction framework of mechanical structures using a power density theory: Application to off-road vehicle front axle housing. Measurement, 220, 113352.

[4] Venturini, S., Rosso, C., & Velardocchia, M. (2024). An automotive steel wheel digital twin for failure identification under accelerated fatigue tests. Engineering Failure Analysis, 158, 107979.

[5] Heindel, L., Hantschke, P., & Kästner, M. (2023). Fatigue monitoring and maneuver identification for vehicle fleets using a virtual sensing approach. International Journal of Fatigue, 170, 107554.

[6] Heindel, L., Wendrock, F., Hantschke, P., et al. (2023). Economic fatigue damage monitoring for vehicle fleets using the scattering transform. PAMM, 23(4), e202300192.

[7] Jiang, F., Ding, Y., Song, Y., et al. (2021). Digital twin-driven framework for fatigue life prediction of steel bridges using a probabilistic multiscale model: Application to segmental orthotropic steel deck specimen. Engineering Structures, 241, 112461.

[8] Nhamage, I. A., Dang, N.-S., Horas, C. S., et al. (2023). Performing fatigue state characterization in railway steel bridges using digital twin models. Applied Sciences, 13(11), 6741.

[9] Li, D., Chen, Q., Wang, H., et al. (2024). Deep learning-based acoustic emission data clustering for crack evaluation of welded joints in field bridges. Automation in Construction, 165, 105540.

[10] Ma, Y., Liu, M., Yang, L., et al. (2025). Monitoring of weld damage based on deep learning and acoustic emission methods. Journal of Constructional Steel Research, 231, 109583.

[11] Zhu, L., Guo, H., Song, Z., et al. (2025). Machine learning-based fatigue life prediction for E36 steel welded joints. Materials, 18(15), 3481.

[12] Chen, S., Bai, Y., Zhou, X., et al. (2024). A deep learning dataset for metal multiaxial fatigue life prediction. Scientific Data, 11(1), 1027.

[13] Deng, C., Luo, C., Gong, B., et al. (2025). A dataset of fatigue properties for welded joints. Scientific Data, 12(1), 1815.

[14] Hamada, A., Elyamny, S., Abd-Elaziem, W., et al. (2025). Advancing fatigue life prediction with machine learning: A review. Materials Today Communications, 43, 111525.

[15] Yang, C., Yang, L., Guo, W., et al. (2023). Deep learning-based structural damage identification for the strain field of a subway bolster. Alexandria Engineering Journal, 81, 264 – 283.

[16] Sadeghian, E., Dragomirescu, E., & Inkpen, D. (2025). Damage detection for a cantilevered steel I-beam using deep learning methods: LSTM, multivariate time-series transformer, and LSTM-based autoencoder. Journal of Computing in Civil Engineering, 39(2), 04025003.

[17] Zhang, C., Wan, R., He, J., et al. (2025). A multiaxial fatigue life analysis method for automotive components based on LSTM-CNN. International Journal of Fatigue, 199, 109062.

[18] Lin, Y.-Z., Nie, Z.-H., & Ma, H.-W. (2022). Dynamics-based cross-domain structural damage detection through deep transfer learning. Computer-Aided Civil and

Infrastructure Engineering, 37(1), 24 – 54.

[19] Wang, X., & Xia, Y. (2022). Knowledge transfer for structural damage detection through re-weighted adversarial domain adaptation. Mechanical Systems and Signal Processing, 172, 108991.

[20] Giglioni, V., Poole, J., Venanzi, I., et al. (2024). A domain adaptation approach to damage classification with an application to bridge monitoring. Mechanical Systems and Signal Processing, 209, 111135.

[21] Lu, N., Xiao, X., Cui, J., et al. (2025). An unsupervised cross-domain method for bridge damage detection based on multichannel symmetric dot pattern feature alignment. Computer-Aided Civil and Infrastructure Engineering, 40(29), 5698 – 5718.

[22] Lei, Y., Li, J., & Hao, H. (2024). Physics-guided deep learning based on modal sensitivity for structural damage identification with unseen damage patterns. Engineering Structures, 316, 118510.

[23] Schubnell, J., Fliegener, S., Rosenberger, J., et al. (2025). Data-driven fatigue assessment of welded steel joints based on transfer learning. Welding in the World, 69(8), 2223-2238.

[24] Shi, S., Yao, D., Wu, G., et al. (2024). Characterization of fatigue damage in Hadfield steel using acoustic emission and machine learning-based methods. Sensors, 24(1), 275.

[25] Liu, J., Xu, Y., Cao, M., et al. (2023). Fatigue crack size evaluation using acoustic emission signals for wire and arc additive manufactured materials. Mechanical Systems and Signal Processing, 204, 110819.